



Vaasan yliopisto
UNIVERSITY OF VAASA

OSUVA Open
Science

This is a self-archived – parallel published version of this article in the publication archive of the University of Vaasa. It might differ from the original.

Risk-based Peer-to-peer Energy Trading with Info-Gap Approach in the Presence of Electric Vehicles

Author(s): Seyyedeh-Barhagh, Sahar; Abapour, Mehdi; Mohammadi-Ivatloo, Behnam; Shafie-khah, Miadreza

Title: Risk-based Peer-to-peer Energy Trading with Info-Gap Approach in the Presence of Electric Vehicles

Year: 2023

Version: Accepted manuscript

Copyright ©2023 Elsevier. This manuscript version is made available under the Creative Commons Attribution–NonCommercial–NoDerivatives 4.0 International (CC BY–NC–ND 4.0) license, <https://creativecommons.org/licenses/by-nc-nd/4.0/>

Please cite the original version:

Seyyedeh-Barhagh, S., Abapour, M., Mohammadi-Ivatloo, B. & Shafie-khah, M. (2023). Risk-based Peer-to-peer Energy Trading with Info-Gap Approach in the Presence of Electric Vehicles. *Sustainable Cities and Society* 99, 104948. <https://doi.org/10.1016/j.scs.2023.104948>

Risk-based Peer-to-peer Energy Trading with Info-Gap Approach in the Presence of Electric Vehicles

Sahar Seyyedeh Barhagh^{1,2}, Mehdi Abapour^{1,*}, Behnam Mohammadi-Ivatloo^{1,3}, Miadreza Shafiekhah²

¹ Faculty of Electrical and Computer Engineering, University of Tabriz, Tabriz, Iran

² School of Technology and Innovations, University of Vaasa, Vaasa, Finland

³ Department of Electrical Engineering, LUT University, Lappeenranta, Finland

* Corresponding author

Abstract – Small-scale smart microgrid is prone to economic consideration of adequate transactive energy sharing and reliable certified power pool hub. Moreover, direct integration of efficient with renewable energy providers in presence of storage such as electric vehicle (EV) aggregation improves the performance of energy systems and guarantees secure trade among the consumers. However, unified modeling of the energy community framework faces the challenge of load management. In this paper, an optimal risk management procedure is proposed for renewable-based presumes such as photovoltaic (PV), and EV to maximize the horizon of uncertainty parameter. The energy demand in peer to peer (P2P) household energy sharing is considered as the uncertain parameter. To this end, in order to study the behavior of a risk-averse and a risk-seeker decision-maker, an information-gap decision theory (IGDT) probability model is applied. In order to demonstrate the performance of the proposed approach, the model is implemented in a test microgrid and the simulation results are presented and discussed.

Keywords – Peer to peer (P2P) trading, risk management, electric vehicle (EV), information gap decision theory (IGDT).

Nomenclature

H	The number of complexes
T	The horizon for scheduling
λ_t^G	The cost of importing electricity from the grid upstream
$P_{t,h}^G$	Imported from the upstream grid.
$P_{t,h}^L$	Each complex's load
$P_{t,h}^{G,L}$	The imported power from the upstream network to satisfy each complex's demand
$P_{t,h}^{P2P,L}$	The quantity of electricity exchanged between complexes

$P_{t,h}^{Dch,L}$	The EVPL's discharge power
$P_{t,h}^{PV,L}$	The solar panel's generated electricity
$P_{t,h}^G$	The overall quantity of power imported from the upstream network
$P_{t,h}^{G,L}$	The upstream grid's exported power to satisfy each complex demand
$P_{t,h}^{G,Ch}$	The upstream grid's exported energy used to charge EVs parked at the EVPL
$P_{t,h}^{PV}$	The total power produced by the PV unit
$P_{t,h}^{PV,L}$	Each complex is supplied with imported power from a PV system
$P_{t,h}^{PV,P2P}$	The PV unit's produced energy used for peer-to-peer trading
$P_{t,h}^{PV,Ch}$	The PV unit's generated power used to charge the EVs parked at the EVPL
$P_{t,h}^{Ch}$	The total power stored in the batteries of EVs that are parked in the EVPL
$P_{t,h}^{P2P,Ch}$	The P2P trading power for charging the EV's parked in the EVPL
$P_{t,h}^{Dch}$	The total amount of discharging power of EVs' battery
$P_{t,h}^{Dch,L}$	The amount of EV battery discharging power required to meet each complex's demand
$P_{t,h}^{Dch,P2P}$	The amount of the EV battery's discharge power for P2P trade
$SOC_{t,h}$	The stored energy level at the current time interval
η^{G2V}, η^{V2G}	The EVPL's charging and discharging efficiency
N_h^{EV}	The number of EVs that are parked in the EVPL
$P_{Max}^{Ch}, P_{Max}^{Dch}$	EVPL's maximum charge and discharge limits
$\alpha_{t,h}^{Ch}, \alpha_{t,h}^{Dch}$	The auxiliary variables employed to indicate the operation mode of EVPL
$Z_{t,h}$	A parameter to indicate the availability of EVs in the EVPL
ΔSOC^{EV}	The different SOC of EV between two consecutive hours
Δ_{SOC}^{Max}	The maximum SOC difference limitation between two consecutive hours

$P_{t,h}^{P2P,In}$	Each complex's total input power
$P_{t,h}^{P2P,O}$	The total amount of each complex output
K	A big number
$\mu_{t,h}^{P2P,In}$	An auxiliary binary variable
α	The boundary of uncertainty
C_r	Referred to as the microgrid's critical cost
C_0	The deterministic value of the optimum cost of the microgrid
C_p	Defined as the target cost of the microgrid

27

28 **1. Introduction**

29 Nowadays, due to the concerns about air pollution, which is mainly caused by fossil fuel power
30 plants, most consumers have decided to supply their demands by distributed energy resources to
31 be self-sufficient and have clean air. However, in some circumstances, the output power of
32 prosumers is more than their requirement. On the other hand, due to several reasons, such as lack
33 of access to battery storage or insufficient storage capacity, the generated power inevitably could
34 be wasted by distributed energy resources. Recently, implementing a peer-to-peer (P2P) trading
35 method has partially solved this problem by selling extra generated power of houses to the houses,
36 requiring more energy (Suthar et al., 2023). The significance of P2P energy trading method is
37 demonstrated in (Espadinha et al., 2023) where a P2P optimization model was created to evaluate
38 the P2P role for decarbonizing Portugal by 2050. In this study, it is assumed that each of the 278
39 considered municipalities should create an energy community with four competitive sectors as
40 players.

41 At the Portuguese national level, expenses and CO₂ emissions decreased under the communal self-
42 consumption and P2P scenarios, respectively. Moreover, the services sector emerged as an active

43 trader, with the biggest volume of energy sold on the P2P market, while the residential sector
44 clearly displayed buyer and seller behavior.

45 Through employing this method, several goals can be achieved. For instance, surplus generated
46 power would not waste and the homeowner; who has surplus generated power; can gain economic
47 benefit by selling it to other consumers. To recapitulate, this indicates the effectiveness of the
48 proposed method and decreases the dependency of microgrids from the upstream network as much
49 as possible (Soto et al., 2021; Tushar et al., 2021).

50 In this part, a review of recent works and research activities on P2P energy trading is presented.
51 A novel P2P market structure based on a multi-bilateral economic dispatch (MBED) is presented
52 in (Sorin et al., 2019), where the relaxed consensus+innovation (RCI) approach is utilized to solve
53 the studied problem. By implementing this method, social welfare is maximized besides
54 considering consumer performance. Likewise, in (Tushar et al., 2019), a motivational game-
55 theoretic approach is employed for P2P energy trading in a smart grid to reach some targets such
56 as the reduction of carbon emissions and the energy cost, encouraging the users for participating
57 in the energy trading. To help the centralized power system to decrease the total electricity demand
58 of customers at the peak hour, a P2P energy trading scheme is implemented by formulating the
59 cooperative Stackelberg game in (Tushar et al., 2020). Authors in (Siano et al., 2019) have studied
60 the concept of energy as a new consensus protocol for P2P energy exchange management. In order
61 to decrease the power peaks in critical time periods, a subscription-based tariff structure is
62 presented in (Almenning et al., 2019). A prediction-integration trading optimization model for
63 prosumers in the continuous double auction-based electricity market is implemented in (Chen et
64 al., 2019) to improve the prosumer profit in different market situations and increase the market

65 transaction rate. In another study, for solving the energy-sharing problem, a two-stage energy-
66 sharing strategy is developed to result in economic benefits in energy buildings (Cui et al., 2019).
67 In (Hahnel et al., 2020), Huhnel et al have focused on customer preferences in P2P energy trading.
68 They have tried to make the extent homeowners more clear regarding their behavior as well as
69 their conditions in the P2P energy trading system. The main aim of this study is to enhance the
70 amount of P2P trading in decentralized energy systems. According to their analysis of German
71 homeowners, it is shown that the main factors of homeowners' trading behavior are the state of
72 charge of private storage units and the electricity prices of the community. In order to achieve the
73 benefits as well as decrease the need for sensing and communication infrastructures in P2P energy
74 sharing, a two-stage control method is applied in (Long et al., 2018). In this work, each prosumer
75 is allowed to control its distributed energy resources through a third-party entity. Besides that, the
76 authors in (Melendez et al., 2019) have proposed a new method to investigate the improvement of
77 the end-user consumers from aggregation and develop some rules in order to minimize the cost of
78 the system. To survey the feasibility of renewable sources like PV systems in P2P energy trading
79 and evaluate the economic benefit, an optimization model is applied in (Nguyen et al., 2018).
80 Valuable good guidelines and a review of some recent works about the real blockchain-based
81 electricity market are studied in (Wörner et al., 2019). In (Talari et al., 2022), a fully decentralized
82 market mechanism is proposed that respects prosumers' preferences, including their readiness to
83 trade renewable energy, the reputation of their trading partners, and their position within the
84 network. Powerful consumers are encouraged to participate in the market on their own while
85 maintaining their privacy.

86 Both uncertainty trading and energy trading are considered in the P2P local electricity market
87 model in (Zhang et al., 2020). In order to increase participation in the reserve market, ref.

88 (Bjarghov et al., 2019) have proposed a three-stage stochastic market-clearing model, where real-
89 time markets, and internal intraday are cleared properly considering the uncertainty of load and
90 activation of reserves. The employment of game-theoretic approaches for P2P energy trading is
91 studied and various games and auction theoretic approaches are proposed for providing
92 information about the systematic classification in (Tushar et al., 2018). The authors of (Zepter et
93 al., 2019) have studied integrating prosumer communities into the existing day-ahead and intraday
94 markets, where a stochastic programming approach was developed in two levels to enhance the
95 economic performance of the P2P trade and battery storage.

96 The integration of P2P energy sharing with demand-side management was put forth in (Zhao
97 et al., 2023) for energy management. In order to guarantee that every household could fairly
98 participate in P2P sharing and take advantage of cheap PV electricity, it adopted a uniform price
99 and energy allocation method based on the ratio of supply to demand. A multi-objective
100 optimization strategy was utilized to find the scheduling scheme for flexible loads when
101 community members engage in P2P sharing. On the structure of this model, the uncertainty and
102 the employment of EV is disregarded.

103 The authors in (Xia et al., 2023) proposed a P2P energy trading mechanism that included a
104 preference marginal price and an uncertainty local marginal price (LMP). Although this paper
105 considers the uncertainty of the renewable energy recourses at the first step, it does not consider
106 the load uncertainty. In (Haider et al., 2022), a centralized optimization algorithm is used in P2P
107 energy trading procedure, which is encouraged by pricing factors considering EV charging and
108 discharging behaviors. In this paper, EVs have been considered but there is not any renewable
109 energy resource and the existing uncertainties have not been taken into account.

110 According to (Hutty et al., 2021), a local microgrid of 50 households with penetrations of PV
111 and EV has been modeled by a P2P energy trading platform. The authors in this work employed
112 the P2P concept with unidirectional EV chargers and chargers that can discharge EV battery energy
113 to the home or the grid; the usage of energy storage has been taken into consideration. However,
114 the uncertainty of the consumers' load is not managed in this work which can affect the strategy
115 of the decision-maker.

116 A P2P energy trading platform for prosumers has been introduced as a generalized aggregative
117 game in (Belgioioso et al., 2022), where a network operator is in charge of enforcing the system's
118 operating limitations. A distributed market-clearing mechanism has been employed in this paper.
119 However, in the designation of this model, there are not any EVs, PVs, and uncertainty.

120 In (Yang et al., 2022), a Stackelberg game model was used to account for the interaction
121 between the prosumers trading energy in a P2P market and the grid operator. On the prosumer side,
122 distributed renewable generators and energy storage technologies are taken into account. The bi-
123 level optimization issue generated by the Stackelberg game has been transformed into a single-
124 level mixed-integer quadratic programming (MIQP) by examining the problem structures in order
125 to address the difficulties of finding the network fee price. The difference of this paper with our
126 research is that the authors did not consider EVs and also the uncertainty of the load has been
127 ignored.

128 Network-constrained P2P energy trading scheme for multiple microgrids under uncertainty has
129 been addressed in (Liu et al., 2023). A bi-level optimization framework has been presented to make
130 a connection between the P2P transactions under uncertainty and physical power flows monitored
131 by distribution system operators. To reduce power losses and ensure the operational security of
132 local distribution networks, an upper-level conditional optimum power flow model is developed.

133 A stochastic programming-based P2P trading model for multiple microgrids is developed at a
134 lower level. A nested bi-level distributed algorithm with a parallel analytical target cascading
135 algorithm and an alternating direction multiplier method are created to solve the model in a
136 distributed manner while realizing the consistency of decision-making processes between the two
137 levels and among various microgrids. The authors in this paper do not consider any renewable
138 energy resources that can enhance the flexibility of the P2P energy trading framework.

139 In (Fernandez et al., 2021), an energy management system for a community is assumed that
140 enables P2P energy trading between customers with renewable energy units, a central storage
141 facility, and a power grid. Two optimization frameworks for distributing extra on-site generated
142 energy are established. Whereas in the first framework, a game theoretical model, maximizes
143 consumer utilization at the lower level and the revenue of the common storage facility at the higher
144 level, the second framework maximizes the combined revenue of sellers and purchasers. The
145 difference of this paper with our paper is that not only EVs but also the load's uncertainty has been
146 neglected.

147 According to the studied literature review, it can be observed that the P2P energy trading scheme
148 is beneficial to the power system but appears to be challenging at the same time. In P2P
149 transactions, purchasers are expected to trade their required demand independently and directly
150 from the peer suppliers, which imposes a notable amount of uncertainty into the P2P energy trading
151 platform. Therefore, encouraging the prosumers and consumers to participate in such an
152 environment with significant uncertainty in the amount of the traded demand is a challenging task.
153 Therefore, the model of energy transactions in a P2P manner should be considered in handle of
154 these challenges to manage the risk associated with the amount of consumer consumption is
155 necessary, while minimizing the cost of the whole P2P energy trading platform. The uncertainty

156 in the P2P energy trading platforms is one of the most critical issues; especially the uncertainty
 157 originating from the amount of the load of the end-users; that should be taken into account which
 158 are neglected in (Belgioioso et al., 2022; Fernandez et al., 2021; Zhao et al., 2023). Moreover, the
 159 employment of EVs in the energy system can provide more flexibility to the end-users to
 160 participate in the P2P transactions which are not given proper attention or are neglected totally in
 161 (Belgioioso et al., 2022; Fernandez et al., 2021; Yang et al., 2022).

162 A taxonomy table is presented to compare a number of the recent models with the proposed
 163 framework. It should be noted that there are a few models that considered the uncertainty in the
 164 management of the P2P frameworks; however, no efficient strategy is provided for managing the
 165 system operation against the demand uncertainty. As the cost of the framework could be reduced
 166 if an accurate risk-management model for handling the uncertainty posed by the demand of the
 167 participants is chosen. In fact, in order to take appropriate actions against this kind of uncertainty,
 168 optimal operating strategies are required to be provided. Moreover, analyzing the source of
 169 uncertainty in the P2P framework from different perspectives is also another key point that
 170 provides beter viewpoint to the decision-maker to choose the best strategy against the demand
 171 uncertainty.

172 Table 1: A taxonomy table comparing a number of P2P energy trading platforms.

Ref.	Clean production		Uncertainty	Risk management from different perspectives	Objective
	EV	PV			
(Zhao et al., 2023)	✗	✓	✗	✗	Minimizing the overall cost of the community
(Haider et al., 2022)	✓	✗	✗	✗	Reducing network congestion
(Belgioioso et al., 2022)	✗	✗	✗	✗	Maximizing the safety and reliable operation of the system
(Yang et al., 2022)	✗	✓	✗	✗	Maximizing the economy benefits.
(Liu et al., 2023)	✗	✗	✓	✗	Minimizing power losses and guaranteeing the operating security of local distribution networks.

(Fernandez et al., 2021)	✘	✓	✘	✘	Maximizing consumer utilization at the lower level and the revenue of the common storage facility at the higher level.
(Hutty et al., 2021)	✓	✓	✘	✘	Maximizing the penetration of PVs and EVs
(Xia et al., 2023)	✘	✓	✓	✘	Minimizing the operation cost
Our model	✓	✓	✓	✓	IGDT-based risk-constrained models corresponding to the demand uncertainty are formulated in the robust and opportunistic structures

173

174 In order to resolve the issues expressed in the studied literature review, this paper develops an
175 Information gap decision theory (IGDT) based optimization framework for studying the
176 performance of a local operator in a microgrid connected to the main network under demand
177 uncertainty. Using the IGDT, this model was precisely formulated to address both robust and
178 opportunistic behaviors in dealing with uncertainties. The obtained results from this approach can
179 be used by the local operator to apply the appropriate operating strategies within various
180 uncertainty levels. Different aspects of demand uncertainty are taken into account in the IGDT
181 method and then according to the desired targets for the risk-averse and risk-seeker decisions, the
182 provided strategies are applied to determine the best possible configurations for the local operator
183 under different uncertainty levels.

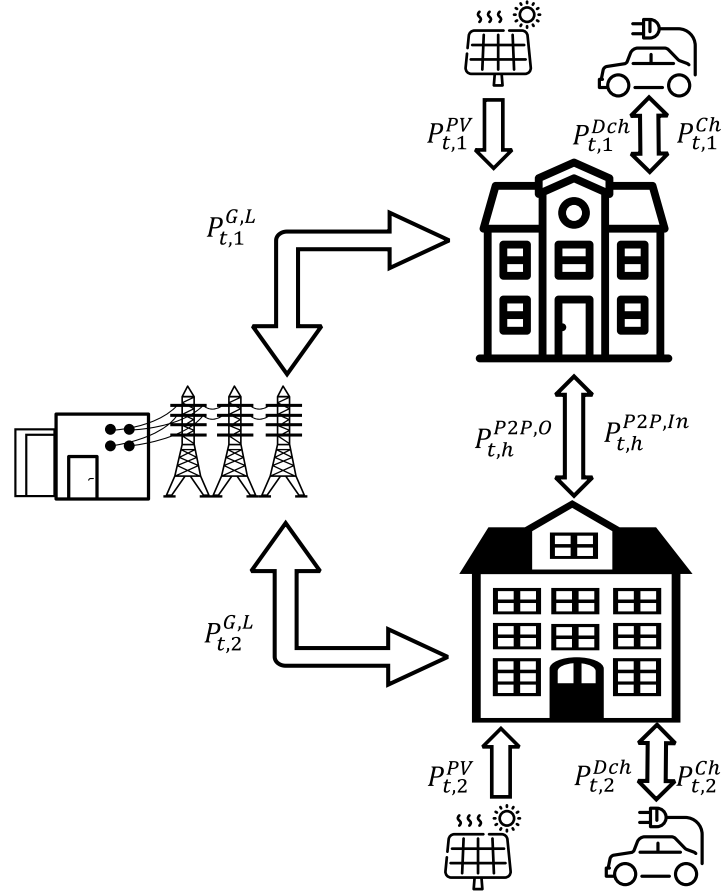
184 The rest of the paper is organized as follows: Section 2 is dedicated to the problem formulation.
185 The Uncertainties are discussed in Section 3. The results and required input data are presented in
186 Section 4. Finally, the conclusions of this paper are provided in Section 5.

187

188 2. Problem formulation and constraints

189 In this section, the mathematical formulation associated with P2P energy trading in a renewable
190 grid-connected microgrid system is presented. In order to explain the decision variables in the
191 proposed model, a schematic of the framework is depicted in Fig. 1. According to Figure 1, the

192 studied system represents an energy framework interconnected with the upstream power grid,
193 enabling a bidirectional flow of electric power. Additionally, two prosumers involved in the system
194 possess the capability to engage in P2P energy trading, which further empowers the system's
195 energy flexibility. Each prosumer is equipped with an EV parking lot and renewable energy
196 resources, i.e. PV solar panels. The primary function of the prosumers in this system is to fulfill
197 the power requirements of their own demand through the upstream grid, the PV panels, and the
198 EV parking lot. During certain hours, if the prosumers have surplus power that is not required,
199 they have the option to engage in P2P energy transactions with another peer. Alternatively, they
200 can choose to sell their excess power to the upstream network. Moreover, the EVs within the
201 system also possess the ability to engage in a bidirectional power exchange. This energy-sharing
202 mechanism optimizes the utilization of available resources and enhances the overall energy
203 efficiency of the system. The employed decision variables shown in this figure are explained and
204 discussed in detail.



205

206

Fig. 1. The schematic of the proposed P2P framework.

207 *2.1. Objective function*

208 As the objective function, the total cost of the system including the cost of power purchase from
 209 upstream grid, should be minimized (1).

$$Obj = Min \sum_{t=1}^T \sum_{h=1}^H P_{t,h}^G \lambda_t^G \quad (1)$$

210 where: *Obj* is the objective function, *H* is the number of complexes, *h* is the complex index, *T* is

211 the scheduling horizon, *t* is the time index, $P_{t,h}^G$ is imported power from the upstream network, λ_t^G is

212 the price of power imported from the upstream grid.

213 *2.2. Energy balance constraint*

214 According to the power balance constraint in the studied system (2), the energy demand should be
 215 met with the traded energy, grid power, generated power by renewables and the charge/discharge
 216 of EVPL.

$$P_{t,h,s}^L = P_{t,h}^{G,L} + P_{t,h}^{P2P,L} + P_{t,h}^{Dch,L} + P_{t,h,s}^{PV,L} \quad \forall t, \forall h \quad (2)$$

217 where: $P_{t,h}^L$ is the load of each complex, $P_{t,h}^{G,L}$ is the imported power from the upstream network
 218 for meeting the demanded power of each complex, $P_{t,h}^{P2P,L}$ is the trading power between complexes,
 219 $P_{t,h}^{Dch,L}$ is the discharge power of EVPL, $P_{t,h}^{PV,L}$ is the generated power of the PV unit, respectively.

220 2.3. Generation Supply

221 To meet the energy demand, each complex supply power from the upstream network, PV unit and
 222 EVPL.

223 2.3.1. Power Grid

224 Energy is purchased from the upstream network to supply energy demand in each complex and
 225 charge the EVs parked in the EVPL, as expressed (3).

$$P_{t,h}^G = P_{t,h}^{G,L} + P_{t,h}^{G,Ch} \quad \forall t, \forall h \quad (3)$$

226 where $P_{t,h}^G$ is the total amount of imported power from the upstream network, $P_{t,h}^{G,L}$ is the exported
 227 power from the upstream grid to meet each complex demand, $P_{t,h}^{G,Ch}$ and is the exported power
 228 from the upstream grid to charge EVs parked in the EVPL.

229 2.3.2. Photovoltaic (PV) units

230 Generated power of PV is used for supplying each complex demand, P2P trading, and charging
 231 the EVs parked in the EVPL, as expressed in (4).

$$P_{t,h,s}^{PV} = P_{t,h,s}^{PV,L} + P_{t,h,s}^{PV,P2P} + P_{t,h,s}^{PV,Ch} \quad \forall t, \forall h \quad (4)$$

232 where $P_{t,h,s}^{PV}$ is the total amount of generated power of PV unit in time t , complex h and scenario s ,
 233 $P_{t,h,s}^{PV,L}$ is the imported power from PV system to each complex, $P_{t,h,s}^{PV,P2P}$ is the generated power of
 234 PV unit for P2P trading and $P_{t,h,s}^{PV,Ch}$ is the generated power of PV unit for charging the EVs parked
 235 in the EVPL.

236 2.3.3. Electric Vehicle Parking Lots

237 The equations (5)-(6) present the charging and discharging power of the EVs parked in the EVPL.
 238 In (5) the battery of parked EVs in the EVPL is charged by upstream network, traded P2P energy
 239 and PV unit.

$$P_{t,h}^{Ch} = P_{t,h}^{G,Ch} + P_{t,h}^{P2P,Ch} + P_{t,h}^{PV,Ch} \quad \forall t, \forall h \quad (5)$$

240 where $P_{t,h}^{Ch}$ is the total amount of power in the battery of p EVs parked in the EVPL, $P_{t,h}^{P2P,Ch}$ is the
 241 P2P trading power for charging the EV's parked in the EVPL. The battery of parked EVs in the
 242 EVPL is discharged for meeting the load demand of each complex and P2P trading (6).

$$P_{t,h}^{Dch} = P_{t,h}^{Dch,L} + P_{t,h}^{Dch,P2P} \quad \forall t, \forall h \quad (6)$$

243 where $P_{t,h}^{Dch}$ is the total amount of discharging power of EVs' battery, $P_{t,h}^{Dch,L}$ is the discharging
 244 power of EVs' battery to meet the load demand of each complex, $P_{t,h}^{Dch,P2P}$ is the discharging
 245 power of EVs' battery for P2P trading.

246 2.4. Operation of Electric Vehicle Parking Lot

247 The operation of EVPL is modeled according to (7)-(13). The state of charge (SOC) of EVPL is
 248 expressed in (7), where the SOC at each time is dependent on the SOC at previous hour and the
 249 charge/discharge power.

$$SOC_{t,h} = SOC_{(t-1)h} + \left(P_{t,h}^{EVP,Ch} \eta^{G2V} - \frac{P_{t,h}^{EVP,DCh}}{\eta^{V2G}} \right) N_h^{EV} \quad \forall (t > 1), \forall h \quad (7)$$

250 In the above constraint, $SOC_{t,h}$ is the stored energy level at the current time interval, η^{G2V} and η^{V2G}
 251 are the charging and discharging efficiencies of the EVPL and N_h^{EV} is the number of parked EVs
 252 in the EVPL.

$$SOC_{t,h} = SOC^{ini} + \left(P_{t,h}^{EVP,Ch} \eta^{G2V} - \frac{P_{t,h}^{EVP,Dch}}{\eta^{V2G}} \right) N_h^{EV} \quad \forall (t = 1), \forall h \quad (8)$$

253 According to (9), the energy stored in the battery of parked EVs in the EVPL must be within the
 254 technically specified capacity of EVPL.

$$SOC_h^{min} \leq SOC_{t,h} \leq SOC_h^{max} \quad \forall t, \forall h \quad (9)$$

255 The SOC of EVs in the EVPL at the departure time should satisfy the desired SOC for each EV,
 256 as expressed in (10).

$$SOC_{t,h} \geq SOC_h^{Des} \quad \forall t = Dep \quad (10)$$

257 The charging/discharging power constraints of EVPL are expressed in (11)-(12).

$$P_{t,ch}^{Ch} \leq P_{Max}^{Ch} \alpha_{t,h}^{Ch} Z_{t,h} \quad \forall t, \forall h \quad (11)$$

$$P_{t,ch}^{Dch} \leq P_{Max}^{Dch} \alpha_{t,h}^{Dch} Z_{t,h} \quad \forall t, \forall h \quad (12)$$

258 where P_{Max}^{Ch} and P_{Max}^{Dch} are the maximum charge and discharge limitations of EVPL, $\alpha_{t,h}^{Ch}$ and
 259 $\alpha_{t,h}^{Dch}$ are the auxiliary variables employed to indicate the operation mode of EVPL, $Z_{t,h}$ is a
 260 parameter to indicate the availability of EVs in the EVPL. It should be also noted that of electric
 261 vehicle parking lots (EVPL) cannot be charged and discharged operationally at the same time, as
 262 presented in constraint (13).

$$\alpha_{t,h}^{Ch} + \alpha_{t,h}^{Dch} \leq Z_{t,h} \quad \forall t, \forall h \quad (13)$$

263 The ΔSOC^{EV} is the different SOC of EV between two consecutive hours, which is limited in (14).

264 Note that Δ_{SOC}^{Max} is the maximum SOC difference limitation between two consecutive hours.

$$-\Delta_{SOC}^{Max} \leq SOC_{t,h} - SOC_{(t-1),h} \leq \Delta_{SOC}^{Max} \quad \forall (t > 1), \forall h \quad (14)$$

265 2.5. Peer-to-peer (P2P) energy trading

266 The traded power between the complexes is expressed in (15)-(23). According to these constraints,
 267 received/delivered power by each complex is a combination of shared/received powers by other
 268 complexes.

269 Each complex trades with other complexes as a definition of P2P trading to meet its demand and
 270 charge the batteries of parked EVs in the EVPL, as expressed in (15).

$$P_{t,h}^{P2P,In} = P_{t,h}^{P2P,Ch} + P_{t,h}^{P2P,L} \quad \forall t, \forall h \quad (15)$$

271 where $P_{t,h}^{P2P,In}$ is the total amount of input power of each complex. According to the equation (16),
 272 the output of each complex depends on the amount of discharging the EVs' battery and the amount
 273 of power generation of PV unit.

$$P_{t,h}^{P2P,O} = P_{t,h}^{Dch,P2P} + P_{t,h}^{PV,P2P} \quad \forall t, \forall h \quad (16)$$

274 Where: $P_{t,h}^{P2P,O}$ is the total amount of each complex output. The output power of each complex is
 275 equal to the input power of other complexes in the P2P trading, as expressed in (17)-(18).

$$P_{t,h=1}^{P2P,In} = P_{t,h=2}^{P2P,O} \quad \forall t \quad (17)$$

$$P_{t,h=1}^{P2P,O} = P_{t,h=2}^{P2P,In} \quad \forall t \quad (18)$$

276

277 The total amount of trading power in the P2P trading of each complex should be equal with other
 278 complexes at the end of the day, as expressed in (19).

$$\sum_{t=1}^T P_{t,h}^{P2P,In} = \sum_{t=1}^T P_{t,h}^{P2P,O} \quad \forall h \quad (19)$$

279 Simultaneous import and export of energy via P2P energy trading is limited (20)-(21).

$$P_{t,h}^{P2P,In} \leq K \mu_{t,h}^{P2P,In} \quad \forall t, \forall h \quad (20)$$

$$P_{t,h}^{P2P,O} = K(1 - \mu_{t,h}^{P2P,In}) \quad \forall t, \forall h \quad (21)$$

280

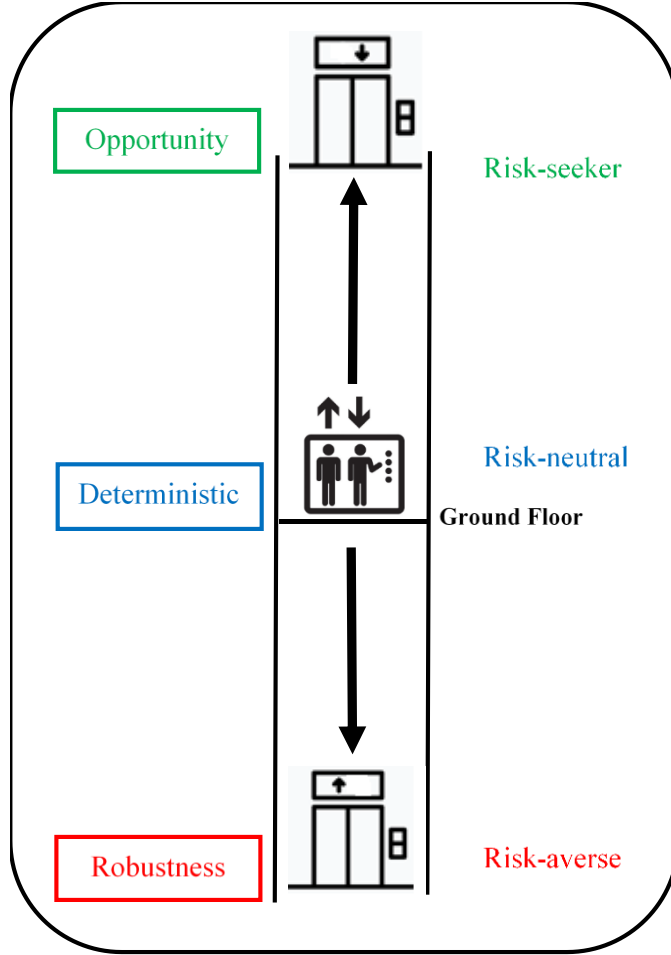
281 where: K is a big number and $\mu_{t,h}^{P2P,In}$ is an auxiliary binary variable to avoid import and export
282 power among complexes in P2P trading simultaneously.

283 3. Uncertainty modeling

284 Most of the time, due to endless uncertainties and lack of access to needed information by
285 operators, they are unable to plan the operation of power systems for the future properly and
286 accurately. To solve this problem, the authors decided to make an almost accurate prediction for
287 the future by modeling these uncertainties with different methods. One of these uncertainties is the
288 output power of solar cells because this parameter is mainly dependent on environmental
289 conditions, and these conditions are constantly changing. In this paper, for modeling the output
290 power of PV, series of scenarios based on the historical data are generated. And, to model another
291 of the uncertainty that is the injected load of complexes from the network in the exciting microgrid
292 as well as the electricity price for the energy purchased from the upstream grid, the IGDT is used
293 to investigate a variety of cases from worst to best for reaching proper strategy.

294 IGDT is a decision-making framework that takes into account the impact of uncertainty on a
295 system. It provides a way to model and analyze decision problems in the presence of incomplete
296 or limited information. Figure 2 is depicted to address this concept in detail. In this figure, which
297 represents a lift diagram, the different levels of the lift correspond to the different approaches taken
298 to address uncertainty. When the lift is on the 0 floor, it signifies that the impact of uncertainty is
299 neglected. Thus, we are in the deterministic mode. At this level, it is assumed that there are no
300 uncertain parameters affecting the decision-making process. In other words, the decision-maker
301 assumes that they have complete information and can accurately assess the outcomes and risks
302 associated with their choices.

303 However, as the lift moves to higher levels, it indicates that the decision-maker acknowledges
304 the existence of uncertainty and incorporates it into their decision-making process. Therefore, the
305 opportunity function of IGDT method is used to evaluate the potential benefits that can be derived
306 from uncertainty. Being on higher levels implies that the decision-maker is willing to take risks
307 and seeks to exploit the uncertainty for possible gains. On the other hand, when the lift descends
308 to levels below 0, it signifies that the robust function of IGDT is being employed. The robust
309 function models the negative impacts of uncertainty, and the decision-maker aims to make their
310 model resistant against these negative effects. By being on lower levels, the decision-maker
311 demonstrates risk aversion and prioritizes safeguarding their system against the potential negative
312 effects of uncertainty. Hence, the levels of the lift in Figure 2 represent the different attitudes of
313 the decision-maker towards uncertainty. Higher levels indicate a risk-seeking behavior, where
314 uncertainty is seen as an opportunity for potential benefits. Conversely, lower levels indicate risk-
315 averse behavior, where the decision-maker focuses on protecting the system from the negative
316 impacts of uncertainty through the application of the robustness function of the IGDT approach.



317

318

Fig. 2. The concept of the robustness and opportunity functions of information-gap approach

319

3.1. Robustness function of IGDT based method:

320

A risk-averse decision-maker uses the robustness function of the IGDT framework in order to find

321

the maximum horizon of the uncertainty of the uncertain parameters which are the electricity price

322

and load. This function is formulated as follows:

$$\hat{\alpha}(q, C_r) = \text{Maximize } \alpha \quad (22)$$

323

s.t:

$$C^* = \text{Max} \left(\sum_{t=1}^T \sum_{h=1}^H P_{t,h}^G \lambda_t^G \right) \leq C_r = (1 + \omega)C_0 \quad (23)$$

$$(1 - \alpha)\tilde{\lambda}_t^G \leq \lambda_t^G \leq (1 + \alpha)\tilde{\lambda}_t^G \quad (24)$$

$$(1 - \alpha)\tilde{P}_{t,h}^L \leq P_t^L \leq (1 + \alpha)\tilde{P}_{t,h}^L \quad (25)$$

$$(2) - (21) \quad (26)$$

324 In the above formulation, α is the horizon of the uncertainty. The main goal of this formulation
 325 is maximizing the optimum value of the uncertain horizon while guaranteeing that the microgrid
 326 cost in the robustness mode, i.e., C^* will not exceed the critical cost of the microgrid (C_r). It should
 327 be noted that C_r is equal to $C_r = (1 + \omega)C_0$ and C_0 is the deterministic value of the optimum cost
 328 of the microgrid. In this mathematical formulation, ω is the cost variation factor that is employed
 329 to set the risk averseness of the microgrid operator. It is an input parameter between 0 and 1. As
 330 the decision-maker becomes more risk-averse against the uncertain parameter, higher values for
 331 the cost deviation factor should be chosen. Constraints (24) and (25) indicate that the fractional
 332 uncertainty model for IGDT approach is used (Jasinski et al., 2023). In the above formulation, the
 333 maximum value for the microgrid cost will occur if the highest electrical load $P_{t,h}^L$ and electricity
 334 price λ_t^G would be selected as the uncertain parameters. Therefore, constraints (29) and (30) can
 335 be easily replaced by $\lambda_t^G = \tilde{\lambda}_t^G(1 + \alpha)$ and $P_{t,h}^L = \tilde{P}_{t,h}^L(1 + \alpha)$. Hence, the problem formulation
 336 can be simplified as follows:

$$\hat{\alpha}(q, C_r) = \text{Maximize } \alpha \quad (27)$$

337 s.t:

$$C^* \leq C_r = (1 + \omega)C_0 \quad (28)$$

$$\lambda_t^G = \tilde{\lambda}_t^G(1 + \alpha) \quad (29)$$

$$P_{t,h}^L = \tilde{P}_{t,h}^L(1 + \alpha) \quad (30)$$

$$(2) - (21) \quad (31)$$

338 The solution of this optimization problem will provide the optimum horizon of the demand
 339 uncertainty for risk-averse decision-maker under different levels of the deviation factor, i.e. ω .

340 3.2. Opportunity function of IGDT based method:

341 Behavior of the risk-seeker decision-maker is being analyzed through an opportunity function
 342 based on the IGDT approach. This function is formulated as:

$$\hat{\beta}(q, C_p) = \text{minimize } \alpha \quad (32)$$

343 s.t:

$$C^{\angle} = \min \left(\sum_{t=1}^T \sum_{h=1}^H P_{t,h}^G \lambda_t^G \right) \leq C_p = (1 - \omega)C_0 \quad (33)$$

$$(1 - \alpha)\tilde{\lambda}_t^G \leq \lambda_t^G \leq (1 + \alpha)\tilde{\lambda}_t^G \quad (34)$$

$$(1 - \alpha)\tilde{P}_{t,h}^L \leq P_{t,h}^L \leq (1 + \alpha)\tilde{P}_{t,h}^L \quad (35)$$

$$(2) - (21) \quad (36)$$

344 In the opportunity strategy of the IGDT approach, the main objective of this model is
 345 minimizing the optimum value of the uncertain horizon while guaranteeing that the microgrid cost
 346 in the opportunity mode, i.e., C^{\angle} might be lower than the target cost of the microgrid (C_p), where
 347 C_p is equal to $C_p = (1 - \omega)C_0$ and C_0 is the deterministic value of the optimum cost of the
 348 microgrid. In other words, the opportunity function is used to determine the possible reduction of
 349 microgrid cost due to low load consumption. Thus, the low values for α is preferred. In the above
 350 formulation, the minimum value for the microgrid cost will occur if the lowest electrical load $P_{t,h}^L$
 351 and electricity price λ_t^G would be consumed as the uncertain parameters. Therefore, constraints
 352 (34) and (35) can be easily replaced by $\lambda_t^G = \tilde{\lambda}_t^G(1 + \alpha)$ and $P_{t,h}^L = \tilde{P}_{t,h}^L(1 - \alpha)$. Hence, the
 353 problem formulation can be simplified as follows:

$$\hat{\beta}(q, C_p) = \text{minimize } \alpha \quad (37)$$

354 s.t:

$$C^L \leq C_p = (1 - \omega)C_0 \quad (38)$$

$$\lambda_t^G = \tilde{\lambda}_t^G(1 + \alpha) \quad (39)$$

$$P_{t,h}^L = \tilde{P}_{t,h}^L(1 - \alpha) \quad (40)$$

$$(2)-(21) \quad (41)$$

355 The solution of this optimization problem will provide the optimum horizon of the demand
 356 uncertainty for risk seeker decision-maker under different levels of the deviation factor, i.e. ω .

357 4. Simulations

358 In this section, risk-based performance of local operator against the uncertainty of demand and
 359 electricity price is studied in a test system shown in Fig. 3. As it can be seen, there are two
 360 residential complexes, the complexes are connected to the upstream grid which is illustrated as a
 361 conventional power plant. Moreover, the PV panels are connected to each complex which covers
 362 a percentage of the demand of the microgrid. Finally, two EV parking lots are considered in this
 363 case that enable the complexes to charge or discharge their EVs. It should be noted that both
 364 complexes have PV solar systems and EV parking lots, demonstrating a shared commitment to
 365 renewable energy integration and sustainable transportation. On the other side, there are
 366 differences in a number of factors such as the energy consumption of each complex, the quantity
 367 of power generated by PV panels, the pattern of charging and discharging EVs in the parking lots.

368 The proposed model in the deterministic stage has a MILP formulation. Thus, the optimization
 369 problems of this stage can be solved by a MILP solver, such as CPLEX used in this paper.
 370 However, it is important to note that the IGDT-based model includes the multiplication of two
 371 variables, which introduces non-linearity into the problem. This nonlinearity in the optimization
 372 model arises from the multiplication of the decision variables, which are the horizon of the
 373 uncertainty to the load and also to the electricity price. Thus, the IGDT-based problem

374 formulations are formulated as mixed-integer non-linear programming (MINLP). The simulations
375 are done using a general algebraic modeling system (GAMS). The DICOPT solver is employed to
376 find the optimum solution and results are illustrated for different levels of uncertainty.

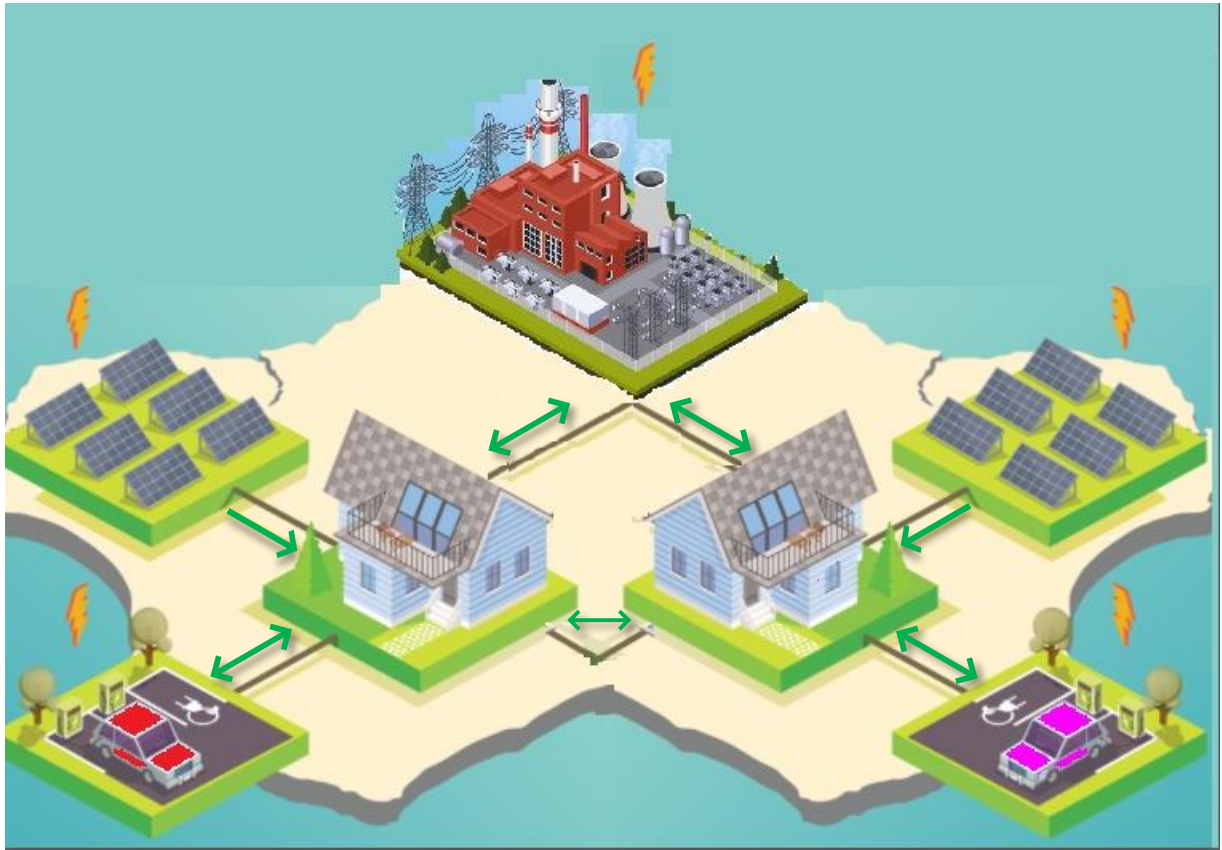
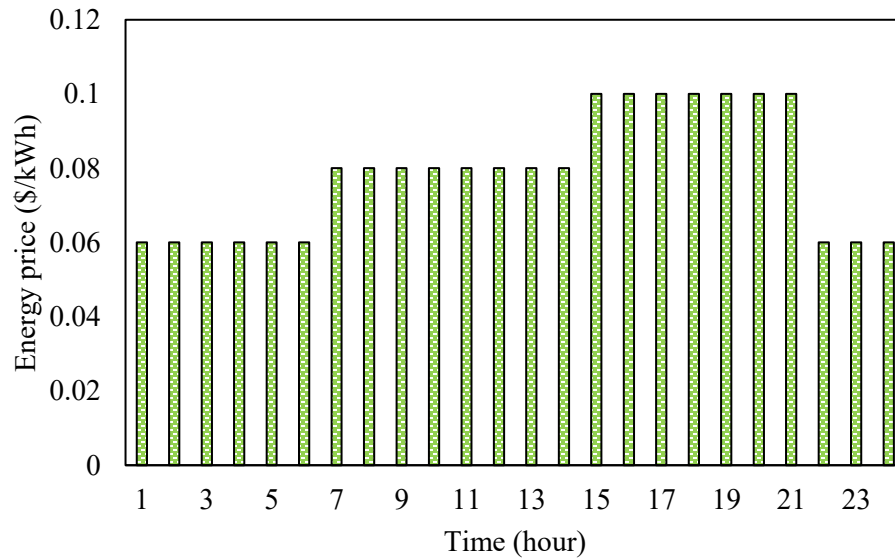


Fig. 3. The structure of the studied test system

377
378
379 *4.1. Input data*

380 Hourly expected electricity prices and expected load profiles are taken from (Zepter et al., 2019).
381 The expected prices are presented in Fig. 4. Then, the reduced generated scenarios regarding the
382 hourly output power of the PV panels are presented in Table 1. Based on the nominal installed
383 capacity of the panels for each complex, the final value is different. The nominal installed
384 capacities of the PV unit of Complex 1 and Complex 2 are 40 kW and 35 kW, respectively.
385 Therefore, the amount of power generated by PV unit in Complex 1 would be higher than that in
386 Complex 2. Furthermore, the arrival and departure patterns of EVs in each EV parking lot are

387 illustrated in Fig. 5. According to this figure, the arrival times of EVs to the EVPLs 1 and 2 are
 388 12:00 and 9:00. While their departure times from the parking lots are 8:00 and 17:00.



389

390

Fig. 4. The expected energy price s over the studies period

391

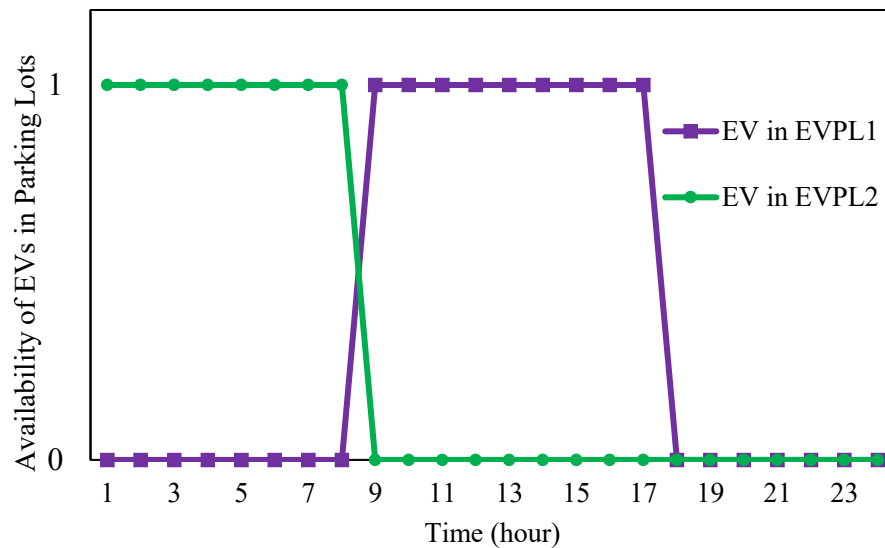
392

Table 2: The generation scenarios of PV panels

S T	9	2	3	4	5	6	7	8	1	10	11	12	13	14	15
1	0	0	0	0	0	0	0	0	0	0	0	0	0	0	0
2	0	0	0	0	0	0	0	0	0	0	0	0	0	0	0
3	0	0	0	0	0	0	0	0	0	0	0	0	0	0	0
4	0	0	0	0	0	0	0	0	0	0	0	0	0	0	0
5	0.095	0.089	0.082	0.094	0.089	0.09	0.093	0.084	0.085	0.1	0.089	0.103	0.081	0.093	0.069
6	0.511	0.316	0.412	0.404	0.424	0.41	0.403	0.464	0.417	0.522	0.418	0.45	0.438	0.455	0.424
7	0.684	0.89	0.82	0.729	1.058	0.889	1.065	0.969	0.77	0.947	0.954	0.938	0.917	0.834	0.972
8	1.241	1.059	1.23	1.212	1.068	1.043	1.125	1.242	1.014	1.121	1.048	1.21	1.079	1.238	0.894
9	1.49	1.888	1.622	1.71	1.627	1.703	1.742	1.807	1.8	1.809	1.679	1.66	1.661	1.604	2.091
10	1.904	1.974	1.919	1.641	1.745	1.65	1.26	1.723	2.084	1.867	1.829	1.782	1.708	1.81	1.938
11	1.535	1.747	1.829	1.778	1.516	1.716	1.647	1.487	1.837	1.569	1.791	1.685	1.801	1.602	1.314
12	2.069	1.636	2.018	1.967	1.691	1.397	1.815	1.909	1.752	1.463	1.716	1.774	1.823	1.839	1.805
13	1.374	1.129	1.191	1.027	0.983	1.406	1.1	1.195	1.237	1.062	1.065	1.119	1.341	1.134	1.096
14	0.752	0.719	0.714	0.655	0.726	0.64	0.76	0.569	0.662	0.797	0.685	0.728	0.751	0.624	0.737
15	0.685	0.681	0.811	0.878	0.813	0.739	0.695	0.787	0.765	0.865	0.761	0.757	0.668	0.639	0.689
16	0.876	0.81	0.752	0.757	0.661	0.728	0.777	0.697	0.791	0.618	0.681	0.716	0.604	0.757	0.724

17	0.606	0.756	0.765	0.746	0.658	0.682	0.737	0.606	0.695	0.648	0.695	0.823	0.729	0.657	0.652
18	0.302	0.405	0.37	0.334	0.309	0.392	0.365	0.415	0.302	0.365	0.337	0.391	0.326	0.352	0.347
19	0.064	0.075	0.066	0.068	0.063	0.075	0.073	0.065	0.064	0.071	0.081	0.072	0.058	0.06	0.078
20	0	0	0	0	0	0	0	0	0	0	0	0	0	0	0
21	0	0	0	0	0	0	0	0	0	0	0	0	0	0	0
22		0	0	0	0	0	0	0	0	0	0	0	0	0	0
23		0	0	0	0	0	0	0	0	0	0	0	0	0	0
24		0	0	0	0	0	0	0	0	0	0	0	0	0	0

393



394

395

Fig. 5. The departure and arrival patterns of EVs in EVPL

396

397

398

399

400

401

402

403

The technical data of EV parking lots is presented in Table 3 (Jannati & Nazarpour, 2017) and (Seyyedeh Barhagh et al., 2020). This table provides crucial information regarding the specifications and characteristics of the EVPLs utilized in the studied system. It includes essential parameters such as maximum and minimum state of the charging, i.e., SOC_h^{Max} and SOC_h^{min} which represent the upper and lower limits of the battery's charge level, indicating the range within which the EVPL can operate effectively. Moreover, the EVPL's charging and discharging efficiency (η^{G2V} and η^{V2G}) shows the effectiveness of the EVPL which indicate the conversion rate of the electrical energy to charge the battery during the charging process and convert stored energy into electricity

404 power during the discharging process. The other parameters shown in Table 2 are the EVPL's
 405 maximum charge and discharge limits (P_{Max}^{Ch} and P_{Max}^{Dch}) and the maximum SOC difference
 406 limitation between two consecutive hours; that is ΔSOC^{EV} . This limitation specifies the acceptable
 407 range of SOC variation between consecutive time intervals, ensuring the stability and balance of
 408 the EVPLs' energy levels over time.

409 Table 3: EVPL characteristics

Parameter	SOC_h^{\max}	SOC_h^{\min}	Δ_{soc}^{\max}	P_{Max}^{Ch}	P_{Max}^{Dch}	η^{G2V}	η^{V2G}
[Unit]	kWh	kWh	kWh	kW	kW	%	%
Value	4.5	0	1	1.5	1.5	95	90

410

411 4.2. Results and discussion

412 In this stage, the simulation results and discussion are presented. In the first step, it is assumed
 413 that there is no uncertainty and the microgrid operator has perfect information about the expected
 414 electricity price and load consumption values. This stage is called deterministic stage, i.e., Eqs. (1)
 415 – (22). In other words, it is considered that the forecasted values for these parameters are the same
 416 as the observed ones. In this situation, the proposed model is carried out on the studied case and
 417 the objective function is minimizing the microgrid cost considering the load and electricity price
 418 forecasts which is equal to \$2938. It should be noted that further results about this step are
 419 presented and discussed in the following paragraphs as the risk-neutral strategy. As in the
 420 deterministic mode, the decision-maker is neutral against the risks associated by the uncertain
 421 parameter.

422 Then, in the next step, the uncertainty is taken into account. Therefore, the uncertainty posed
 423 through the load and electricity price is addressed through implementation of IGDT framework.
 424 To this end, IGDT robustness and IGDT opportunity approaches are applied for the risk-averse

425 and risk-seeking strategies, respectively. The main objective of risk-averse strategy is maximizing
426 the horizon of the uncertainty (α) while guaranteeing that the final cost (C^*) will not be greater
427 than the critical cost, i.e. C_r , presented in Eqs. (27) – (31). The risk level in the IGDT approach is
428 the deviation cost denoted by ω which is chosen 0 to 0.5. In order to explain in detail, an arbitrary
429 value for ω is chosen, i.e., 0.2. In this case, the critical microgrid cost will be $C_r = (1 + \omega)C_0 =$
430 $(1 + 0.2) \$2938 = \3525 . In this case, after solving the optimization problem, the optimum
431 IGDT robustness value $\hat{\alpha}(q, C_r)$ will be equal to 0.06. This means if the hourly uncertain
432 parameters in load and price be 6% higher than the expected values (which is worsen than the
433 expected values), the decision-maker is certain that the final microgrid cost will not be higher than
434 \$3525. Therefore, implementing a risk-averse strategy, manages the power supply sources in a
435 way to respond to the increase in the load and electricity prices, which in turn leads to increase the
436 operating cost of complexes 1 and 2, indicating the effectiveness of IGDT method in providing a
437 suitable operation strategy for both complexes.

438 Management of the uncertainty through implementation of IGDT robustness approach imposes
439 cost to the decision-maker. This cost is defined as the robustness cost. The robustness cost for
440 different values of $\hat{\alpha}$ is depicted in Fig. 6. It is obvious from this figure that as the decision-maker
441 desires to be more secure against the higher levels of uncertainty, the robustness cost increases as
442 well. For instance, when $\hat{\alpha} = 0.06$, the robustness cost is equal to \$86.

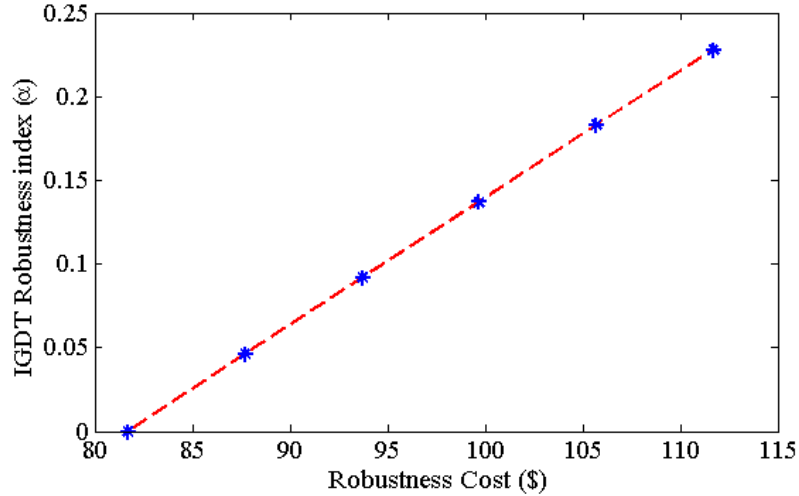


Fig. 6. The robustness cost for different robustness indexes

443

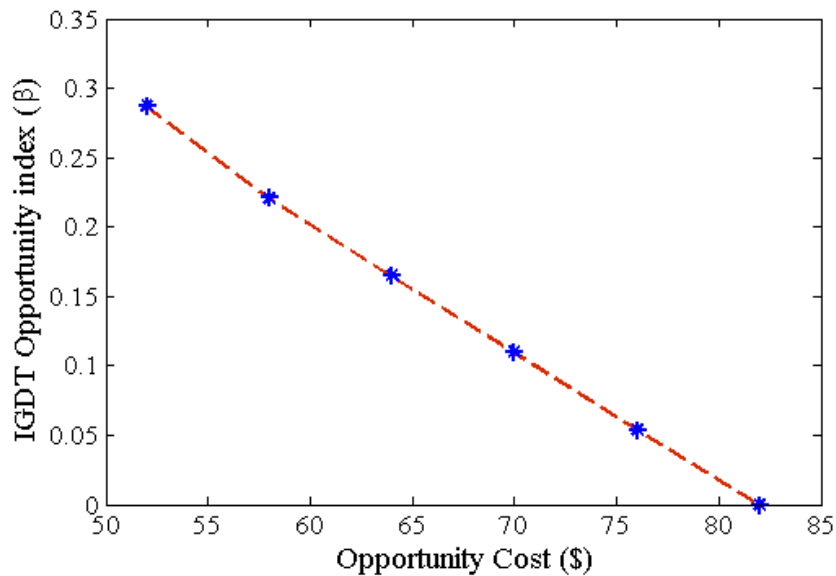
444

445 The impact of IGDT robustness approach on the risk-averse decision-making procedure is
 446 investigated in the previous paragraphs. Now, the risk-seeking strategy is investigated on the
 447 considered test system, presented in Eqs. (37) – (41). The main objective of this method is finding
 448 the minimum value of the uncertain horizon $\hat{\beta}(q, C_p)$ which if the load and prices deviate favorably
 449 in that amount, the decision-maker might reach to lower final microgrid cost (C^{\leftarrow}) than the target
 450 cost (C_p). Similar to the risk-averse strategy, different risk- levels are chosen, $\omega \in$
 451 $\{0, 0.1, 0.2, 0.3, 0.4, 0.5\}$. The same arbitrary value for the cost deviation factor is also chosen. In
 452 this case, the target cost will be $C_p = (1 - \omega)C_0 = (1 - 0.2)\$2938 = \$2350$. In this case, after
 453 solving the optimization problem, the optimum IGDT opportunity value $\hat{\beta}(q, C_r)$ will be equal to
 454 0.075. Therefore, if the load and the electricity prices would be at least 7.5% lower than the
 455 forecasted values (favorable scenario), the final microgrid cost might be \$2350.

456

457 Similar to robustness cost, application of IGDT opportunity function imposes cost to the final
 458 microgrid cost; called opportunity cost. The opportunity cost for different values of $\hat{\beta}$ is depicted
 459 in Fig. 8. It can be seen that higher tendency for lower target costs will lead to an increase in the
 opportunity cost. For example, when $\hat{\beta} = 0.075$, the opportunity cost is equal to \$69. On the other

460 hand, as shown in Fig. 7, reducing in the electrical load demand and experiencing lower electricity
461 prices decrease the operation cost of complexes. This reduction in the uncertain parameters can
462 provide the system operator to take this opportunity and thus managing the energy resources in an
463 optimal way to reduce the cost.

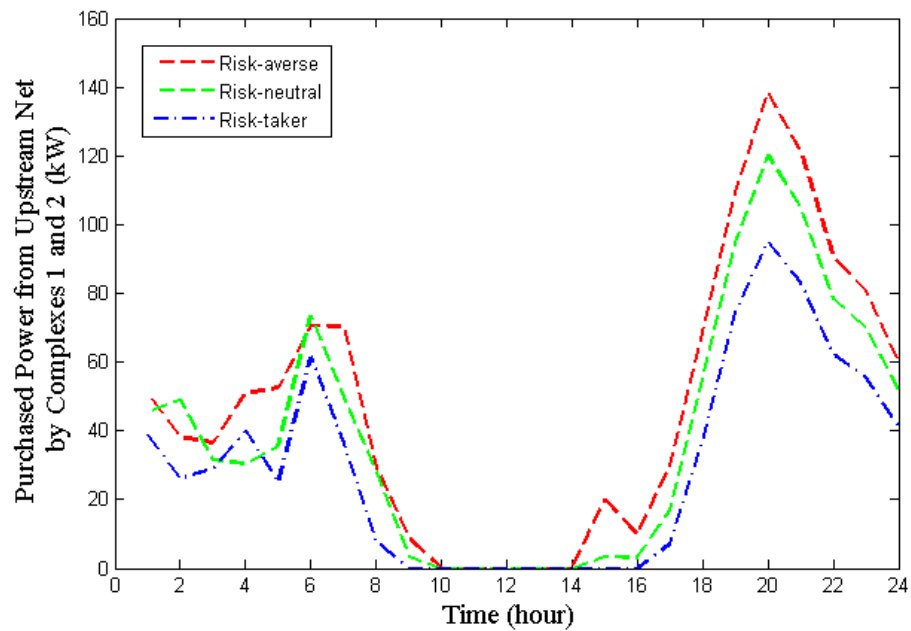


464

465 Fig. 7. The opportunity cost for different opportunity indexes

466 The amount of the purchased power from the upstream grid to meet the electrical load demand
467 of complexes 1 and 2 is depicted in Fig. 8 for three different types of decision-makers such as risk-
468 averse (RA) risk-neutral (RN) and risk-taker (RT). Implementation of the proposed model for
469 different decision makers can provide a clear view of the system's performance under different
470 risk levels. As illustrated, the operator can reduce the purchased power during expensive hours
471 (e.g., 7:00-16:00) by managing the local power generation sources such as PV unit and EVPL. In
472 the early hours of the studied period, the purchased power from upstream network in all risk
473 strategies increase to provide the demand of the complexes 1 and 2, as well as some amount of
474 energy of the EVPL required to charge EVs. The purchased power during these hours increases in
475 the RA mode in order to compensate the load growth under uncertainty. On the other hand, in the

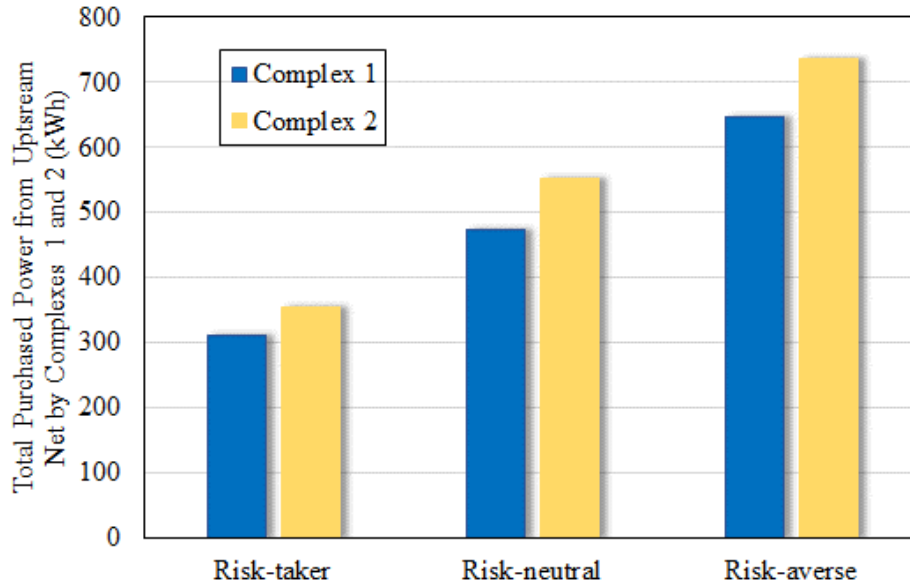
476 semi-peak period (7:00-16:00), the purchased power decreases in all three studied cases. In more
 477 detail, due to the higher price of power during these hours and the load reduction, the purchased
 478 power from the upstream network is close to zero. This shows the efficiency of the proposed model
 479 in using the best strategy for management of the local resources, reduction in the operation cost,
 480 and handling the uncertainties in complexes 1 and 2. According to Fig. 8, in the last hours of the
 481 studied period, the purchased power is proportional to the peak of load demand in complexes 1
 482 and 2. Similarly, in these hours, the operator uses the strategies provided by IGDT method to
 483 provide the required demand under uncertainty in complexes 1 and 2, which reduces the operating
 484 costs in both complexes. Since the strategies designed by IGDT approach allow management of
 485 electrical load in complexes 1 and 2, which leads to the ease of managing the power resources in
 486 the supply side of each residential complex. The total purchased power from the upstream network
 487 to supply the load of each of complexes 1 and 2 in different levels of load uncertainty is shown in
 488 Fig. 9.



489

490

Fig. 8. The purchased power from the upstream grid in complexes for various risk strategies.



491

492 Fig. 9. The total purchased power from the upstream grid in complexes 1 and 2 for various risk strategies.

493 Regarding Figures 10 and 11 which are stating the load profile of the complex 1 and complex

494 2, the consumption of each end-user is dependent to several factors such as the EV charging and

495 discharging period, type of the EV, number of the people living in each complex and the electrical

496 equipment being used. All of these factors result in having a different load profile for the studied

497 case. As shown in these figures, the uncertainty can be considered an unpredictable condition. Due

498 to the uncertainty, the load demand increases in complexes 1 and 2, as shown in red color in Figs.

499 10 and 11. To manage the supply sources and meet energy demand, which is increased due to the

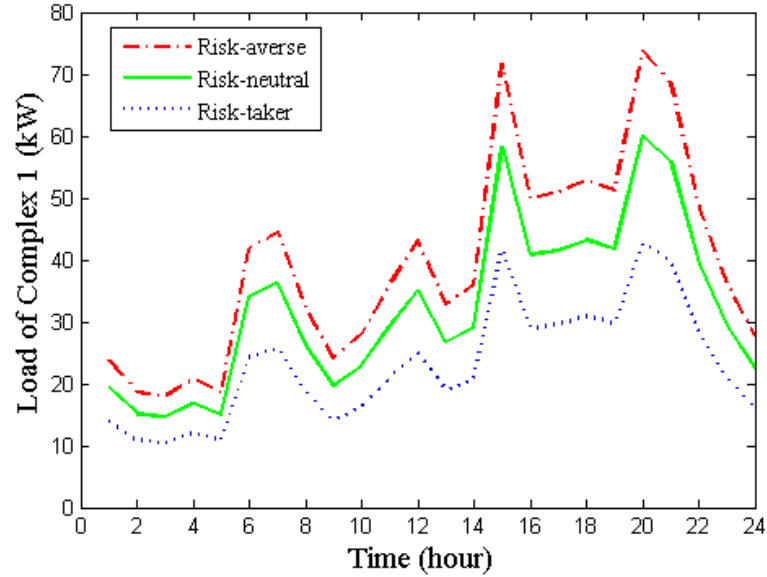
500 uncertainty, the operator can implement a risk-averse strategy. On the other hand, the load demand

501 can decrease due to the uncertainty, as shown in blue. In this case operator can implement risk-

502 taker strategy to manage resources and thus reduce the operation cost of complexes. It is

503 noteworthy that the load demand in normal condition is illustrated in green color in Figs. 10 and

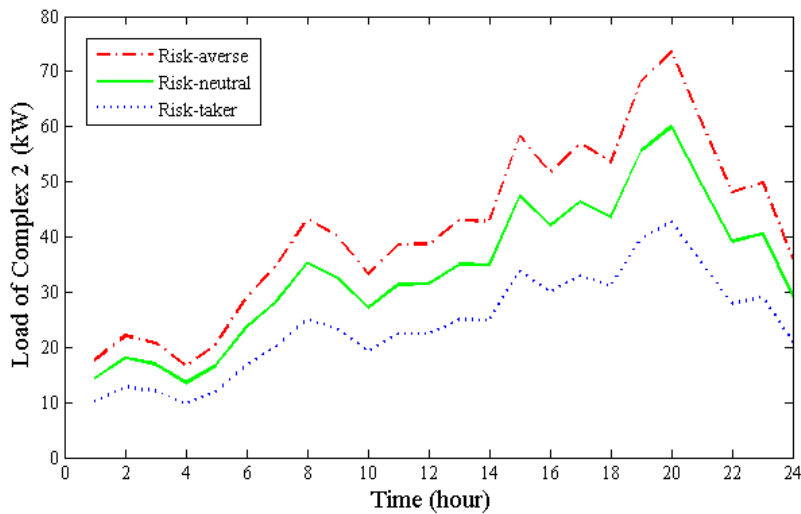
504 11.



505

506

Fig. 10. The load profile of complex 1 in the studied period in three risk strategies



507

508

Fig. 11. The load profile of complex 2 in the studied period in three risk strategies

509

510

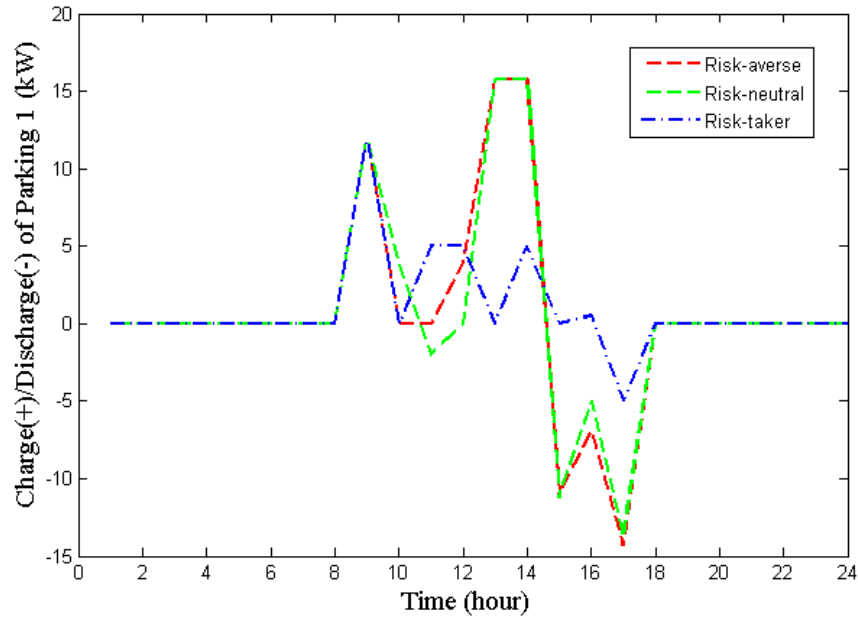
511

512

513

514

The amount of power of EVs in charging and discharging conditions in the EVPL of complexes 1 and 2 are presented in Figs. 12 and 13. In Fig. 12, according to the parking hours of EVs in complex 1, the operator charges EVs in the early hours of the studied period, in which the energy price is low. While in the other hours of the period when the energy price is high, the operator takes advantage of available energy in the EVPL to discharge EVs and balance the electric demand in three different risk strategies (i.e., RA, RN and RT).



515

516

Fig. 12. The SOC of EVPL in complex 1 in three risk strategies

517

518

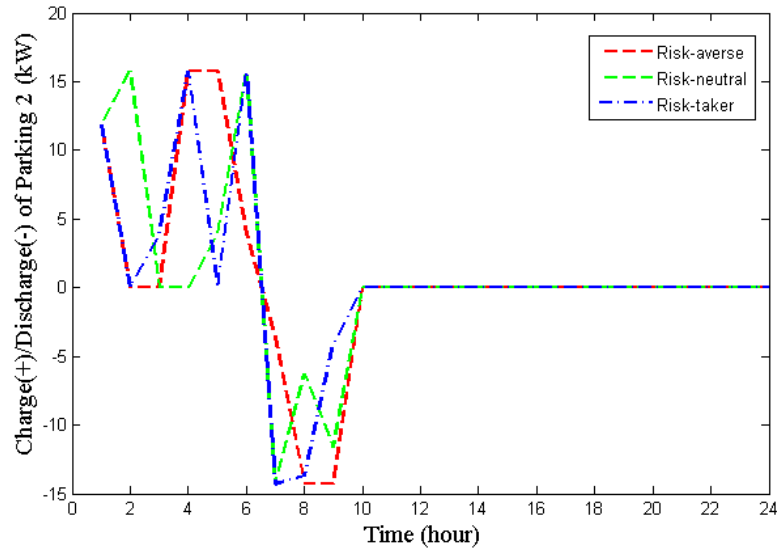
519

520

521

522

In Fig. 13, considering the available charging capacity of EVs in the parking lot, the operator deploys the PV unit to charge the EVs. Once charged, the stored energy is discharged to supply load demand in peak time periods. This shows the efficiency of the proposed model to manage the energy supply sources (i.e., PVs and EVs) and increase the energy efficiency in the operation of studied complexes, which not only avoids loss of energy but also supplies a portion of peak load demand to reduce the operation cost in peak time periods.



523

524

Fig. 13. The SOC of EVPL in complex 2 in three risk modes

525

526

527

528

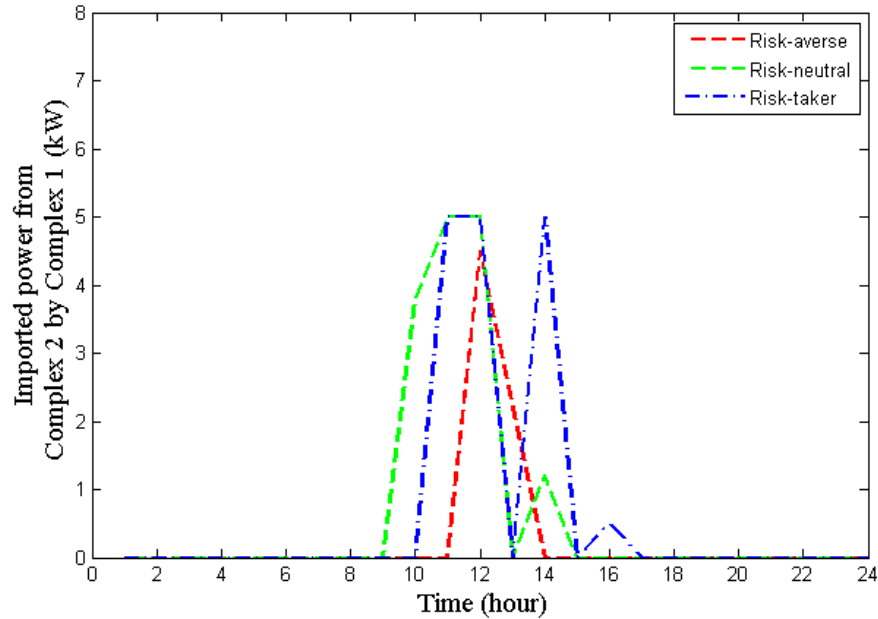
529

530

531

532

Fig. 14 shows the exported power complex 2 to complex 1. In the RA strategy, due to the uncertainty that increases the electric load and price, as well as the limitation of distributed generation resources in complex 2, the exported power to complex 1 decrease. However, in the RT strategy, due to possible reduction in the uncertain parameters, i.e., electric load and price of complex 2, the operator decides to increase the power transfer from complex 2 and supply load demand in complex 1. Moreover, considering the fact that EVs are not available in the EVPL of complex 2 during the day, excess generation by PV unit in this complex is supplied to complex 1 to either serve the load or charge the EVs.



533

534

Fig. 14. The imported power profile from complex 2 to complex 1.

535

536 Our study demonstrated the effectiveness of application of different decision-making strategies
 537 through implementation of the IGDT framework in managing the uncertain parameters. Two
 538 uncertainties are considered in this study, i.e., the electricity prices and the load consumption. The
 539 risk-averse strategy resulted in an increased power purchase from the upstream grid. This decision
 540 was motivated by the desire to mitigate potential negative impacts on the uncertain parameters.
 541 Therefore, the least amount of the P2P transaction accrued when the risk-averse strategy is chosen
 542 happened only in one of the studied hours of the whole period. While the number of hours and
 543 values the risk-taker decision-maker made energy transactions through P2P method with the other
 544 complex is 4 times higher. This can prove the strategy of a risk-taker microgrid operator that seeks
 545 to have lower microgrid costs in case of having a favorable deviation in the observed uncertain
 546 parameters compared to their forecasted values.

547 One of the other most important key findings of the result is related to the costs posed to the
 548 total cost through implementation of the risk-measure, i.e., IGDT. It can be seen that the robustness

549 and opportunity costs are essential to be measured before taking the decision. This cost has a direct
550 relation with the level of risk averseness or willingness. For the lower risk levels, low robustness
551 or opportunity costs are gotten. However, if the operator desires to be secure against the higher
552 deviations of the uncertain parameters, higher costs will be imposed to the total microgrid cost.
553 For instance, if the uncertain parameters deviate 10 unfavorably from the expected values, \$93
554 will be the robustness cost.

555 **5. Conclusion**

556 In this paper, an optimal uncertainty-based operation of a local operator with two energy
557 complexes under the concept of local P2P trading is proposed. The primary objective was to assess
558 the performance of the local operator considering different levels of uncertainty such as risk-
559 neutral, risk-averse, and risk-seeking strategies. To achieve this, IGDT framework was employed
560 to study the effects of uncertainty such as the electrical load and electric price. The findings
561 presented in this work demonstrated that the application of IGDT and the consideration of different
562 decision-making strategies were essential in achieving optimal operation in the face of uncertainty.
563 Thus, the robust function of IGDT was utilized to address uncertainty in the risk-averse mode,
564 where the decision-maker aimed to protect the system against potential negative impacts. In
565 contrast, the opportunity function of IGDT was employed to address uncertainty in the risk-seeking
566 mode, allowing the decision-maker to exploit potential benefits arising from uncertainty.

567 The results revealed distinct behaviors of decision-makers under different strategies. The risk-
568 averse decision-maker showed a willingness to increase purchased power from the upstream grid,
569 maximizing the horizon of uncertainty. This approach aimed to ensure system resilience and
570 minimize potential risks in case of unfavorable deviations on the load and price. On the other hand,
571 the risk-seeking decision-maker adopted an opportunity function of IGDT method by decreasing
572 the purchased power from the upstream grid, aiming for significant cost reductions and targeting

573 on favorable uncertain conditions. Furthermore, we also investigated the operation of other units,
574 such as renewables energy resources and EV parking lots, within the context of optimal P2P local
575 trading in a microgrid. This analysis demonstrated that by employing reasonable strategies,
576 enabled by optimal P2P trading, the overall system performance could be optimized not only in
577 normal operation scenarios but also under uncertainties. For the future directions of the work, the
578 decentralized approach can be investigated in order to examine the dynamics of resource
579 allocation, price negotiation, and the potential benefits of incorporating P2P energy trading in
580 microgrid systems.

581 **References**

- 582 Almenning, O. M., Bjarghov, S., & Farahmand, H. (2019). Reducing Neighborhood Peak Loads with implicit
583 Peer-to-Peer energy trading under Subscribed Capacity tariffs. *SEST 2019 - 2nd International Conference*
584 *on Smart Energy Systems and Technologies*. <https://doi.org/10.1109/SEST.2019.8849067>
- 585 Belgioioso, G., Ananduta, W., Grammatico, S., & Ocampo-Martinez, C. (2022). Operationally-Safe Peer-to-Peer
586 Energy Trading in Distribution Grids: A Game-Theoretic Market-Clearing Mechanism. *IEEE Transactions*
587 *on Smart Grid*. <https://doi.org/10.1109/TSG.2022.3158442>
- 588 Bjarghov, S., Naversen, C. Ø., Thorvaldsen, K., & Farahmand, H. (2019). *A Three-Stage Stochastic Peer-to-*
589 *Peer Market Clearing Model with Real-Time Reserve Activation*.
- 590 Chen, K., Lin, J., & Song, Y. (2019). Trading strategy optimization for a prosumer in continuous double auction-
591 based peer-to-peer market: A prediction-integration model. *Applied Energy*, 242, 1121–1133.
592 <https://doi.org/10.1016/j.apenergy.2019.03.094>
- 593 Cui, S., Wang, Y. W., & Xiao, J. W. (2019). Peer-to-peer energy sharing among smart energy buildings by
594 distributed transaction. *IEEE Transactions on Smart Grid*. <https://doi.org/10.1109/TSG.2019.2906059>
- 595 Espadinha, J., Baptista, P., & Neves, D. (2023). Assessing P2P energy markets contribution for 2050
596 decarbonization goals. *Sustainable Cities and Society*, 92, 104495.
597 <https://doi.org/10.1016/J.SCS.2023.104495>

598 Bernandez, E., Hossain, M. J., Mahmud, K., Nizami, M. S. H., & Kashif, M. (2021). A Bi-level optimization-
599 based community energy management system for optimal energy sharing and trading among peers. *Journal*
600 *of Cleaner Production*. <https://doi.org/10.1016/j.jclepro.2020.123254>

601 Hahnel, U. J. J., Herberz, M., Pena-Bello, A., Parra, D., & Brosch, T. (2020). Becoming prosumer: Revealing
602 trading preferences and decision-making strategies in peer-to-peer energy communities. *Energy Policy*.
603 <https://doi.org/10.1016/j.enpol.2019.111098>

604 Haider, S., Rizvi, R. e. Z., Walewski, J., & Schegner, P. (2022). Investigating peer-to-peer power transactions
605 for reducing EV induced network congestion. *Energy*, 254, 124317.
606 <https://doi.org/10.1016/J.ENERGY.2022.124317>

607 Nutty, T. D., Pena-Bello, A., Dong, S., Parra, D., Rothman, R., & Brown, S. (2021). Peer-to-peer electricity
608 trading as an enabler of increased PV and EV ownership. *Energy Conversion and Management*.
609 <https://doi.org/10.1016/j.enconman.2021.114634>

610 Annati, J., & Nazarpour, D. (2017). Optimal energy management of the smart parking lot under demand response
611 program in the presence of the electrolyser and fuel cell as hydrogen storage system. *Energy Conversion*
612 *and Management*. <https://doi.org/10.1016/j.enconman.2017.02.030>

613 Basinski, M., Najafi, A., Homae, O., Kermani, M., Tsaousoglou, G., Leonowicz, Z., & Novak, T. (2023).
614 Operation and Planning of Energy Hubs Under Uncertainty - A Review of Mathematical Optimization
615 Approaches. *IEEE Access*, 11, 7208–7228. <https://doi.org/10.1109/ACCESS.2023.3237649>

616 Liu, X., Chen, X., Jin, T., Liu, Z., Liu, Y., Su, M., Li, C., & Wu, Q. (2023). Network-Constrained Peer-to-Peer
617 energy trading for multiple microgrids considering zoning pricing. *International Journal of Electrical*
618 *Power & Energy Systems*, 147, 108837. <https://doi.org/10.1016/J.IJEPES.2022.108837>

619 Dong, C., Wu, J., Zhou, Y., & Jenkins, N. (2018). Peer-to-peer energy sharing through a two-stage aggregated
620 battery control in a community Microgrid. *Applied Energy*. <https://doi.org/10.1016/j.apenergy.2018.05.097>

621 Melendez, K. A., Subramanian, V., Das, T. K., & Kwon, C. (2019). Empowering end-use consumers of electricity
622 to aggregate for demand-side participation. *Applied Energy*.
623 <https://doi.org/10.1016/j.apenergy.2019.04.092>

624 Nguyen, S., Peng, W., Sokolowski, P., Alahakoon, D., & Yu, X. (2018). Optimizing rooftop photovoltaic
625 distributed generation with battery storage for peer-to-peer energy trading. *Applied Energy*.
626 <https://doi.org/10.1016/j.apenergy.2018.07.042>

627 Seyyede Barhagh, S., Abapour, M., & Mohammadi-Ivatloo, B. (2020). Optimal scheduling of electric vehicles
628 and photovoltaic systems in residential complexes under real-time pricing mechanism. *Journal of Cleaner*
629 *Production*, 246, 119041. <https://doi.org/10.1016/j.jclepro.2019.119041>

630 Giano, P., De Marco, G., Rolan, A., & Loia, V. (2019). A Survey and Evaluation of the Potentials of Distributed
631 Ledger Technology for Peer-to-Peer Transactive Energy Exchanges in Local Energy Markets. *IEEE*
632 *Systems Journal*. <https://doi.org/10.1109/JSYST.2019.2903172>

633 Sorin, E., Bobo, L., & Pinson, P. (2019). Consensus-Based Approach to Peer-to-Peer Electricity Markets with
634 Product Differentiation. *IEEE Transactions on Power Systems*.
635 <https://doi.org/10.1109/TPWRS.2018.2872880>

636 Oto, E. A., Bosman, L. B., Wollega, E., & Leon-Salas, W. D. (2021). Peer-to-peer energy trading: A review of
637 the literature. *Applied Energy*. <https://doi.org/10.1016/j.apenergy.2020.116268>

638 Uthar, S., Cherukuri, S. H. C., & Pindoriya, N. M. (2023). Peer-to-peer energy trading in smart grid:
639 Frameworks, implementation methodologies, and demonstration projects. *Electric Power Systems*
640 *Research*, 214, 108907. <https://doi.org/10.1016/J.EPSR.2022.108907>

641 Talari, S., Khorasany, M., Razzaghi, R., Ketter, W., & Gazafroudi, A. S. (2022). Mechanism design for
642 decentralized peer-to-peer energy trading considering heterogeneous preferences. *Sustainable Cities and*
643 *Society*, 87, 104182. <https://doi.org/10.1016/J.SCS.2022.104182>

644 Tushar, W., Saha, T. K., Yuen, C., Morstyn, T., McCulloch, M. D., Poor, H. V., & Wood, K. L. (2019). A
645 motivational game-theoretic approach for peer-to-peer energy trading in the smart grid. *Applied Energy*.
646 <https://doi.org/10.1016/j.apenergy.2019.03.111>

647 Tushar, W., Saha, T. K., Yuen, C., Morstyn, T., Nahid-Al-Masood, Poor, H. V., & Bean, R. (2020). Grid
648 Influenced Peer-to-Peer Energy Trading. *IEEE Transactions on Smart Grid*, 11(2), 1407–1418.
649 <https://doi.org/10.1109/TSG.2019.2937981>

650 Ushar, W., Yuen, C., Mohsenian-Rad, H., Saha, T., Poor, H. V., & Wood, K. L. (2018). Transforming energy
651 networks via peer-to-peer energy trading: The potential of game-theoretic approaches. *IEEE Signal*
652 *Processing Magazine*. <https://doi.org/10.1109/MSP.2018.2818327>

653 Ushar, W., Yuen, C., Saha, T. K., Morstyn, T., Chapman, A. C., Alam, M. J. E., Hanif, S., & Poor, H. V. (2021).
654 Peer-to-peer energy systems for connected communities: A review of recent advances and emerging
655 challenges. *Applied Energy*. <https://doi.org/10.1016/j.apenergy.2020.116131>

656 Wörner, A., Meeuw, A., Ableitner, L., Wortmann, F., Schopfer, S., & Tiefenbeck, V. (2019). Trading solar
657 energy within the neighborhood: field implementation of a blockchain-based electricity market. *Energy*
658 *Informatics*. <https://doi.org/10.1186/s42162-019-0092-0>

659 Xia, Y., Xu, Q., Huang, Y., & Du, P. (2023). Peer-to-peer energy trading market considering renewable energy
660 uncertainty and participants' individual preferences. *International Journal of Electrical Power & Energy*
661 *Systems*, 148, 108931. <https://doi.org/10.1016/J.IJEPES.2022.108931>

662 Yang, Y., Chen, Y., Hu, G., & J. Spanos, C. (2022). Optimal Network Charge for Peer-to-Peer Energy Trading:
663 A Grid Perspective. *IEEE Transactions on Power Systems*. <https://doi.org/10.1109/TPWRS.2022.3185585>

664 Zepfer, J. M., Lüth, A., Crespo del Granado, P., & Egging, R. (2019). Prosumer integration in wholesale
665 electricity markets: Synergies of peer-to-peer trade and residential storage. *Energy and Buildings*, 184, 163–
666 176. <https://doi.org/10.1016/j.enbuild.2018.12.003>

667 Zhang, Z., Li, R., & Li, F. (2020). A Novel Peer-to-Peer Local Electricity Market for Joint Trading of Energy
668 and Uncertainty. *IEEE Transactions on Smart Grid*, 11(2), 1205–1215.
669 <https://doi.org/10.1109/TSG.2019.2933574>

670 Zhao, F., Li, Z., Wang, D., & Ma, T. (2023). Peer-to-peer energy sharing with demand-side management for fair
671 revenue distribution and stable grid interaction in the photovoltaic community. *Journal of Cleaner*
672 *Production*, 383, 135271. <https://doi.org/10.1016/J.JCLEPRO.2022.135271>

673

674

